

Spontaneous Flux in a d -wave Superconductor with Time-Reversal-Symmetry-Broken Pairing State at $\{110\}$ Boundaries

J. X. Zhu and C. S. Ting

Department of Physics and Texas Center for Superconductivity, University of Houston, Houston, Texas 77204

Abstract

The induction of an s -wave component in a d -wave superconductor, such as YBCO, is considered. Near the edges of such a sample along $\{110\}$ directions, the induced s -wave order parameter together with d -wave component forms a complex combination $d + e^{i\phi}s$, which breaks the time reversal symmetry (BTRS) of the pairing state. As a result, the spontaneous current is created. We numerically study the current distribution and the formation of the spontaneous flux induced by the current. We show that the spontaneous flux formed from a number of defect lines with $\{110\}$ orientation has a measurable strength. This result may provide a unambiguous way to check the existence of BTRS pairing state at $\{110\}$ boundaries.

PACS numbers: 74.20.-z, 74.25.Jb, 74.50.+r

A distinctive feature of a d -wave superconductor is its sensitivity to inhomogeneities such as impurities, surfaces and interfaces. As one of the nodes of the d -wave energy gap [$\Delta_d(\mathbf{k}) \sim \cos k_x a - \cos k_y a$ in the momentum space] oriented along $\{110\}$ direction is parallel to the normal vector of the surface, Andreev reflected quasiparticles from the surface may experience a sign change in the order parameter. Quantum constructive interference between the incident and Andreev reflected quasiparticle waves then leads to the formation of midgap states [1], which can explain [2,3] the zero-bias conductance peak (ZBCP) observed when tunneling into the $\{110\}$ -oriented thin films [4–6]. Simultaneously, while the d -wave order parameter is suppressed near the surface, a subdominant s -wave component of order parameter may show up. Several authors [7–9] suggested that a broken-time-reversal-symmetry (BTRS) $d + is$ pairing state could be generated near a surface with $\{110\}$ orientation. The prerequisite [9] for the $d + is$ pairing state near such a surface is the presence of a minor s -wave pairing interaction, which is not competitive with the d -channel interaction in the bulk. While the splitting of the ZBCP observed in a copper/insulator/Y-Ba-Cu-O (YBCO) tunneling experiment [10] would be a signature of BTRS pairing state [9,11] formed locally at surfaces, other recent tunneling experiments have observed no such splitting [12–14]. Therefore, the existence of the surface BTRS pairing state in high- T_c superconductors has not been fully established. Since it is a weak and secondary effect relative to the ZBCP in the tunneling experiment, one may argue that the samples [12–14] not showing the splitting could be due to different surface conditions. Here we suggest to measure the spontaneous flux formed near the $\{110\}$ edges as an alternative method to confirm the BTRS pairing state. In this Letter, the spontaneous current distribution or flow pattern in a square d -wave superconductor with $\{110\}$ boundaries will be studied. From this information, we are able to calculate the spontaneous flux distribution near the edges. We show that the total magnetic flux generated by a bunch of defect lines with $\{110\}$ orientation should have a measurable strength. Its observation by experiments will unambiguously indicate the existence of the BTRS pairing state at the $\{110\}$ boundaries.

We first present a preliminary analysis based upon the Ginzburg-Landau (GL) theory to understand how a spontaneous supercurrent is generated by the surface BTRS pairing state in a d -wave superconductor. The GL free energy for a two-component order parameter can be written as

$$\mathcal{F} = \int d^2r \{ \alpha_s |\Delta_s|^2 + \alpha_d |\Delta_d|^2 + \beta_1 |\Delta_s|^4 + \beta_2 |\Delta_d|^4 + \beta_3 |\Delta_s|^2 |\Delta_d|^2 + \beta_4 (\Delta_s^{*2} \Delta_d^2 + \Delta_s^2 \Delta_d^{*2}) + \gamma_s |\mathbf{\Pi} \Delta_s^*|^2 + \gamma_d |\mathbf{\Pi} \Delta_d^*|^2 + \gamma_v [(\Pi_x^* \Delta_s \Pi_x \Delta_d^* - \Pi_y^* \Delta_s \Pi_y \Delta_d^*) + \text{c.c.}] + \frac{(\nabla \times \mathbf{A})^2}{8\pi} \}, \quad (1)$$

where $\Delta_{s,d}^*$ are amplitudes of s - and d -wave components, $\alpha_{s,d}$, β_i ($i = 1, 2, 3, 4$), $\gamma_{s,d,v}$ are real coefficients, \mathbf{A} is the vector potential, $\mathbf{\Pi} = -i\nabla - 2e\mathbf{A}$ is the gauge invariant momentum operator. Note that the free energy here is written in the coordinate system defined by the crystalline a and b axes (i.e., x and y axes in Fig. 1) in YBCO. By varying the free energy with respect to the vector potential \mathbf{A} , we obtain the current

$$\mathbf{J} = 2e \{ \gamma_s \Delta_s \mathbf{\Pi} \Delta_s^* + \gamma_d \Delta_d \mathbf{\Pi} \Delta_d^* + \gamma_v [\Delta_s \mathbf{\Pi}_- \Delta_d^* + \Delta_d \mathbf{\Pi}_- \Delta_s^*] \} + \text{c.c.}, \quad (2)$$

where $\mathbf{\Pi}_- = \Pi_x \mathbf{e}_x - \Pi_y \mathbf{e}_y$ with $\mathbf{e}_{x,y}$ the unit vector along x (y) direction. We take the normal direction of the surface along the \tilde{x} axis and the parallel direction along the \tilde{y} axis. For a

{100} surface where the \tilde{x}, \tilde{y} axes coincide with the a, b crystalline axes, the two components of the order parameter are locked into a real combination $d \pm s$ by the mixed gradient term in the free energy. In this case, no spontaneous current exists. However, for a {110} surface where \tilde{x} and \tilde{y} are respectively along the $y = x$ and $y = -x$ directions as shown in Fig. 1, this mixed gradient term vanishes and an imaginary combination $d \pm is$ is required to minimize the free energy. As a result, we find

$$J_{\tilde{y}} = -4e\gamma_v \text{Im}(\Delta_s \partial_{\tilde{x}} \Delta_d^* + \Delta_d \partial_{\tilde{x}} \Delta_s^*), \quad (3)$$

finite [$J_{\tilde{x}} = 4e \text{Im}(\gamma_s \Delta_s \partial_{\tilde{x}} \Delta_s^* + \gamma_d \Delta_d \partial_{\tilde{y}} \Delta_d^*)$ is identically zero]. Away from the surface towards the bulk, the d -wave component saturates and the s -wave component decays to zero. Thus the parallel spontaneous supercurrent is limited to the surface region. The detailed value of $J_{\tilde{y}}$ must be obtained by solving the GL equation for Δ_s^* and Δ_d^* subject to the boundary conditions. However, the knowledge of $J_{\tilde{y}}$ will not provide the information for the flow pattern since the supercurrent must circulate as loops in a realistic two dimensional system. Although the investigation of supercurrent flow is a challenging topic, it is difficult to employ the GL theory or other continuum theories to examine this problem. Fortunately, the exact diagonalization approach can attack this problem in an elegant way. In addition, the band structure and the short coherence length effects can also be incorporated. The weakness is that the finite size exact diagonalization method, if without modification, lacks the spectral resolution to resolve the resonances in energy. However, for the order parameter and the current (will be calculated below) the finite size effect is small since these two physical quantities are determined by the local pairing interaction and local hopping integral, respectively.

Within the extended Hubbard model, the Hamiltonian on a two-dimensional (2D) square lattice can be written as

$$H = -t \sum_{\langle \mathbf{ij} \rangle \sigma} c_{\mathbf{i}\sigma}^\dagger c_{\mathbf{j}\sigma} - \mu \sum_{\mathbf{i}\sigma} n_{\mathbf{i}\sigma} - V_0 \sum_{\mathbf{i}} n_{\mathbf{i}\uparrow} n_{\mathbf{i}\downarrow} - \frac{V_1}{2} \sum_{\langle \mathbf{ij} \rangle \sigma \sigma'} n_{\mathbf{i}\sigma} n_{\mathbf{j}\sigma'}. \quad (4)$$

Here \mathbf{i} and \mathbf{j} are site indices and the angle bracket implies that the hopping and interactions are only considered up to nearest-neighbor sites, $n_{\mathbf{i}\sigma} = c_{\mathbf{i}\sigma}^\dagger c_{\mathbf{i}\sigma}$ is the electron number operator on site \mathbf{i} , μ is the chemical potential, and t is the hopping integral. The quantities V_0 , and V_1 are on-site and nearest-neighbor interaction strength, respectively. Positive values of V_0 and V_1 mean attractive interactions and negative values mean repulsive interactions. When $V_0 < 0$ and $V_1 > 0$, the d -wave pairing state is favorable. When the above Hamiltonian is examined in the \mathbf{k} -space, it is easy to show that the pairing couplings consist of a dominant d -wave and a minor s -wave interactions.

In the mean-field approximation, the diagonalization of Eq. (4) can be transformed to find the solutions to the lattice Bogoliubov-de Gennes (BdG) equations [15]

$$\sum_{\mathbf{j}} \begin{pmatrix} H_{\mathbf{ij}} & \Delta_{\mathbf{ij}} \\ \Delta_{\mathbf{ij}}^\dagger & -H_{\mathbf{ij}} \end{pmatrix} \begin{pmatrix} u_{\mathbf{j}}^n \\ v_{\mathbf{j}}^n \end{pmatrix} = E_n \begin{pmatrix} u_{\mathbf{i}}^n \\ v_{\mathbf{i}}^n \end{pmatrix}, \quad (5)$$

where $u_{\mathbf{i}}^n$ and $v_{\mathbf{i}}^n$ are the Bogoliubov amplitudes corresponding to the eigenvalue E_n , and

$$H_{\mathbf{ij}} = -t\delta_{\mathbf{i}+\boldsymbol{\delta},\mathbf{j}} - \mu\delta_{\mathbf{ij}}, \quad (6)$$

$$\Delta_{\mathbf{ij}} = \Delta_0(\mathbf{i})\delta_{\mathbf{ij}} + \Delta_{\boldsymbol{\delta}}(\mathbf{i})\delta_{\mathbf{i}+\boldsymbol{\delta},\mathbf{j}}. \quad (7)$$

Here we choose the x and y axes to lie on the diagonals of the sample [as shown in Fig. 1], and $\boldsymbol{\delta} = \pm\hat{\mathbf{x}}, \pm\hat{\mathbf{y}}$ are the nearest-neighbor vectors along the x and y axes. The energy gaps for on-site and nearest-neighbor pairing are determined self-consistently

$$\Delta_0(\mathbf{i}) = V_0 \sum_n u_{\mathbf{i}}^n v_{\mathbf{i}}^{n,*} \tanh(E_n/2T), \quad (8)$$

$$\Delta_{\boldsymbol{\delta}}(\mathbf{i}) = \frac{V_1}{2} \sum_n [u_{\mathbf{i}}^n v_{\mathbf{i}+\boldsymbol{\delta}}^{n,*} + u_{\mathbf{i}+\boldsymbol{\delta}}^n v_{\mathbf{i}}^{n,*}] \tanh(E_n/2T), \quad (9)$$

where the Boltzmann constant $k_B = 1$ has been used. Furthermore, in terms of the Bogoliubov amplitudes, the average of the current operator $J_{\mathbf{ij}} = (-et/\hbar) \sum_{\sigma} [c_{\mathbf{i}\sigma}^{\dagger} c_{\mathbf{j}\sigma} - \text{h.c.}]$ from site \mathbf{j} to \mathbf{i} can be expressed as

$$J_{\mathbf{ij}} = -\frac{2iet}{\hbar} \sum_n \{ [f(E_n)u_{\mathbf{i}}^{n*}u_{\mathbf{j}}^n + (1-f(E_n))v_{\mathbf{i}}^n v_{\mathbf{j}}^{n*}] - \text{c.c.} \}, \quad (10)$$

where the prefactor comes from the spin degeneracy and $f(E) = [\exp(E/T) + 1]^{-1}$ is the Fermi distribution function.

We solve the BdG equations self-consistently by starting with an initial gap function. After exactly diagonalizing Eq. (5), the obtained Bogoliubov amplitudes are substituted into Eqs. (8) and (9) to compute a new gap function. We then use it as input to repeat the above process until the relative error in the gap function between successive iterations is less than a desired accuracy. Throughout our work, we take $V_1 = 3t$, $\mu = -t$. This set of parameter values give the $\Delta_d = 0.368t$, $T_c = 0.569t$, and the corresponding coherence length $\xi_0 = \hbar v_F/\pi\Delta_d \approx 3a$ (In YBCO, $\xi_0 \approx 15 \text{ \AA}$). As a model calculation, the value of hopping integral t will be adjusted to give a reasonable transition temperature.

The amplitudes of the d - and the induced s -wave order parameters are defined as:

$$\Delta_d(\mathbf{i}) = \frac{1}{4} [\Delta_{\hat{\mathbf{x}}}(\mathbf{i}) + \Delta_{-\hat{\mathbf{x}}}(\mathbf{i}) - \Delta_{\hat{\mathbf{y}}}(\mathbf{i}) - \Delta_{-\hat{\mathbf{y}}}(\mathbf{i})], \quad (11a)$$

$$\Delta_s(\mathbf{i}) = \frac{1}{4} [\Delta_{\hat{\mathbf{x}}}(\mathbf{i}) + \Delta_{-\hat{\mathbf{x}}}(\mathbf{i}) + \Delta_{\hat{\mathbf{y}}}(\mathbf{i}) + \Delta_{-\hat{\mathbf{y}}}(\mathbf{i})]. \quad (11b)$$

In general, both components are complex, i.e., $\Delta_{d,s} = |\Delta_{d,s}| \exp(i\phi_{d,s})$ with $\phi_{d,s} \in [0, 2\pi]$. Their relative phase is defined as $\phi = \phi_s - \phi_d$. We first study the spatial variation of s -wave and d -wave order parameter and the relative phase in a square d -wave superconductor having $\{110\}$ boundaries. The obtained current distribution is drawn in Fig. 1. The current direction is denoted by the arrows in the figure. This calculation is made for the sample size $10\sqrt{2}a \times 10\sqrt{2}a$, $T = 0.02t$ and $V_0 = -t$. In addition, the open boundary condition is used. We find that the d -wave order parameter is suppressed near the boundary and approaches to the bulk value beyond a coherence length scale ξ_0 . The induced s -wave component near the boundary oscillates at an atomic scale and decays to zero in the bulk region at a distance

of a few coherence lengths. Near the four corners of the sample, the d -wave component is more strongly suppressed while the magnitude of induced s -wave component is enhanced. Our numerical calculation shows that if the order parameter at site \mathbf{j} within square OHAB (see Fig. 1) is $\Delta_d = d_r - id_i$ and $\Delta_s = s_r + is_i$ [for definiteness, $d_{r,i}$ and $s_{r,i}$ are taken to be positive], then at site \mathbf{j}' within square OHGF which is related to site \mathbf{j} by a $\pi/2$ rotation around the origin O, the order parameter can be obtained as $\Delta_d = d_r + id_i$ and $\Delta_s = -s_r + is_i$. Correspondingly, the relative phase is $\pi/2 + \delta\phi$ at site \mathbf{j} and $\pi/2 - \delta\phi$ at site \mathbf{j}' , where $\delta\phi = \tan^{-1}(s_i/s_r) - \tan^{-1}(d_r/d_i)$ is site dependent. On the $|x| = |y|$ lines [the dotted lines in Fig. 1], $\delta\phi = 0$ and the order parameter becomes exactly $d + is$. Therefore, the pairing state in a square d -wave superconductor with $\{110\}$ boundaries is a BTRS $d + e^{i\phi}s$ state with ϕ varying spatially, and the existence of the BTRS state is limited within a region of the order of ξ_0 near the sample edges. We have also found that the induced s -wave component of order parameter decreases with increasing temperature and on-site repulsive interaction. For a given on-site interaction $V_0 = -t$, the s -component or the surface pairing state vanishes at a temperature about $0.1T_c$. In our lattice model, the current flows into (or out of) each lattice site connecting four bonds. The current conservation on each site is respected. As it can be seen from Fig. 1, the current flowing at four edges, AC, CE, EG, and GA, does not form a closed loop to surround the whole sample. Instead, the current distribution has a spatial reflection symmetry with respect to the x and y axis. Current flows pointing to the corners on the x axis but away from the corners on the y axis. At the left and right corners, the current flowing in the x direction is separated into two equal branches, which flow in the positive and negative y direction; while at the upper and lower corners, the current flowing in the y direction consists of two equal parts flowing in the positive and negative x direction. From an overall point of view, current flows clockwise or counterclockwise in four triangles separated by the x and y axes [i.e., OAC, OAG, OGE, OEC]. Correspondingly, the total flux in two nearest-neighbor triangles for example OAC and OAG has opposite signs. In the upper-right inset of Fig. 1, we indicate the direction of flux in each triangle). In contrast to the regular diamagnetic Meissner current which flows in a penetration depth, the spontaneous current is confined to a distance of a few ξ_0 from the sample edge because it is determined by the spatial variation of order parameter.

To calculate the flux in each triangle, we use the Maxwell equation, $\nabla \times \mathbf{B} = (4\pi/c)\mathbf{J}$, which relates the magnetic field \mathbf{B} to the current density \mathbf{J} . By assuming that the lattice spacing between two consecutive superconducting layers is c_0 , the Maxwell equation can be written as

$$\frac{4\pi}{c}J_{\mathbf{ij}} = \frac{c_0}{a^2}(\Phi_{\mathbf{i}} - \Phi_{\mathbf{j}}), \quad (12)$$

where if \mathbf{ij} is a horizontal link from left to right, $\Phi_{\mathbf{i}}$ and $\Phi_{\mathbf{j}}$ are respectively the magnetic flux passing through the upper and lower plaquettes with the link \mathbf{ij} as a common boundary. The magnetic field and the corresponding flux is perpendicular to the lattice plane since both the current $J_{\mathbf{ij}}$ and the vector connecting the centers of two plaquettes are in the plane. The flux carried by a vortex is then obtained by summing over the flux encircled by each plaquette in a triangle. Using the calculated current distribution to solve Eq. (12), the flux in the triangle AOC is found to be $\Phi = \sum_i \Phi_i = 1.2\mathcal{L}I_0$, where $\mathcal{L} = 4\pi a^2/cc_0$ and $I_0 = et/\hbar$. For $t = 0.014$ eV which gives $T_c \simeq 92.4$ K, and $a = 4$ Å and $c_0 = 10$ Å, we have $\Phi = 4.04 \times 10^{-7}\Phi_0$, where $\Phi_0 = 2.07 \times 10^{-7}$ G · cm² is the superconducting flux quantum.

Due to the small size we consider, the value is too small to be measurable.

To measure the spontaneous flux as an evidence for the BTRS pairing state, we propose the following experiment. Create several long defect lines in a single crystal of d -wave superconductor. These lines lie parallel to the $\{110\}$ direction. For a single defect line of size $6\sqrt{2}a \times \sqrt{2}a$ in a $16a \times 16a$ square lattice, the current distribution is displayed in Fig. 2(a). In this calculation, we use the single-site potential of strength $100t$ making the order parameter with zero magnitude on the defect line, and impose the periodic boundary condition to focus on the effect from the defect line. It should be emphasized that the current is an odd function of position with respect to the defect line. This can also be seen from Eq. (3) by noting that both the d -wave and the induced s -wave components of the order parameter are an even function with respect to the line axis. Therefore, the flux density on both sides has the identical direction and magnitude. In this respect, the system under consideration is different from an s -wave/normal-metal/ d -wave junction [16], where due to the proximity effect, the BTRS pairing state appears in the normal metal region, and the generated spontaneous supercurrent is an even function of position while the spontaneous magnetic flux has opposite sign across the interface. It is this feature that motivates us to suggest the experiment to measure the flux contributed from a number of defect lines. Moreover, because the spontaneous current flows at a distance of the order of coherence length from the defect line, the dominant contribution to the flux is also limited to the same region. Flux direction pointing to the paper near the defect line has been marked by a “+” sign in Fig. 2(a). Note that the flux near BC and AD edges has the same direction as that in the region near AB and CD edges. This is because the width of defect line is too small to exhibit the surface properties. As the length of these two edges is increased, the flux is expected to have an opposite direction relative to that near AB and CD edges. As shown in Fig. 2(b), we can see that the variation of flux trapped by each plaquette along the η line marked in Fig. 2(a) is very small. Therefore, as the defect line is sufficiently long, the flux measured for a segment near the center of line can be approximately estimated as if the ends of defect line do not exist. For this purpose, the spatial variation of current and flux density is plotted in the inset of Fig. 2(b) as the boundary effect from the ends of the defect line is neglected. If the measured length of a defect line is $30 \mu\text{m}$, with the structure parameters taken above, the flux is estimated to be $3.4\% \Phi_0$. When many long defect lines lie parallel to the $\{110\}$ direction and with a spacing of several coherence lengths, the current flowing near each line is almost independent and the total flux is just a simple summation. Consequently, the experimental measurability is greatly enhanced. For example, if there are twenty defect lines, the total flux can be as large as $68\% \Phi_0$. In this sense, the effect of BTRS pairing state is much amplified whereas the information from the tunneling spectroscopy is determined by the local property near one individual defect line or surface. The artificial defect lines can be introduced by heavy-ion bombardment on a thin film of superconductor. With this technique, the edge of the defect line can be very sharp so that it has a well defined in-plane orientation. The magnetic flux can then be measured by a SQUID microscope through a pickup loop. Here the pickup loop should be constructed to cover the central part of all defect lines. Since the proposed experiment does not involve as-grown grain boundaries or twin boundaries, the existence of a spontaneous flux would be a direct evidence for the BTRS pairing state.

We would like to thank Dr. C. C. Tsuei for useful discussions. This work was supported

by the Texas Center for Superconductivity at the University of Houston through a grant from the State of Texas and by the Robert A. Welch Foundation.

REFERENCES

- [1] C. R. Hu, Phys. Rev. Lett. **72**, 1526 (1994).
- [2] Y. Tanaka and S. Kashiwaya, Phys. Rev. Lett. **74**, 3451 (1995).
- [3] J. H. Xu, J. H. Miller, and C. S. Ting, Phys. Rev. B **53**, 3604 (1996).
- [4] J. Geerk, X. X. Xi, and G. Linker, Z. Phys. B **73**, 329 (1988).
- [5] J. Lesueur *et al.*, Physica (Amsterdam) **191C**, 325 (1992).
- [6] M. Covington *et al.*, Appl. Phys. Lett. **68**, 1717 (1996).
- [7] M. Sigrist, D. B. Bailey, and R. B. Laughlin, Phys. Rev. Lett. **74**, 3249 (1995).
- [8] L. J. Buchholtz *et al.*, J. Low Temp. Phys. **101**, 1079 (1995); **101**, 1099 (1995).
- [9] M. Matsumoto and H. Shiba, J. Phys. Soc. Jpn. **64**, 3384 (1995); **64**, 4867 (1995); **65**, 2194 (1996).
- [10] M. Covington *et al.*, Phys. Rev. Lett. **79**, 277 (1997).
- [11] M. Fogelström, D. Rainer, and J. A. Sauls, Phys. Rev. Lett. **79**, 281 (1997).
- [12] S. Sinha and K.-W. Ng, Phys. Rev. Lett. **80**, 1296 (1998).
- [13] A. Engelhardt, R. Dittman, A. I. Braginski, Phys. Rev. B (submitted).
- [14] J. Y. T. Wei, N.-C. Yeh, D. F. Garrigus, and M. Strasik, Phys. Rev. Lett. (to appear).
- [15] P. G. de Gennes, *Superconductivity of Metals and Alloys* (Benjamin, New York, 1966).
- [16] A. Huck, A. v. Otterlo, and M. Sigrist, Phys. Rev. B **56**, 14163 (1997).

FIGURES

FIG. 1. The current distribution in a square d -wave superconductor with $\{110\}$ boundaries. The current direction is represented with arrows. The value of parameters used in the calculation are $T = 0.02t$ and $V_0 = -t$. The upper-right inset shows the direction of flux in each triangle.

FIG. 2. The current distribution near a $\{110\}$ defect line (a) and the spatial variation of flux density along the η line (b). Here η is measured in units of $a' = \sqrt{2}a$ from the line midpoint, $\Phi_c = \mathcal{L}I_0$ with $\mathcal{L} = 4\pi a^2/cc_0$ and $I_0 = et/\hbar$. Inset: Current (solid line) and flux density (dashed line) as a function of distance in units of $a/\sqrt{2}$ from defect line obtained by neglecting the boundary effects from the line's end.

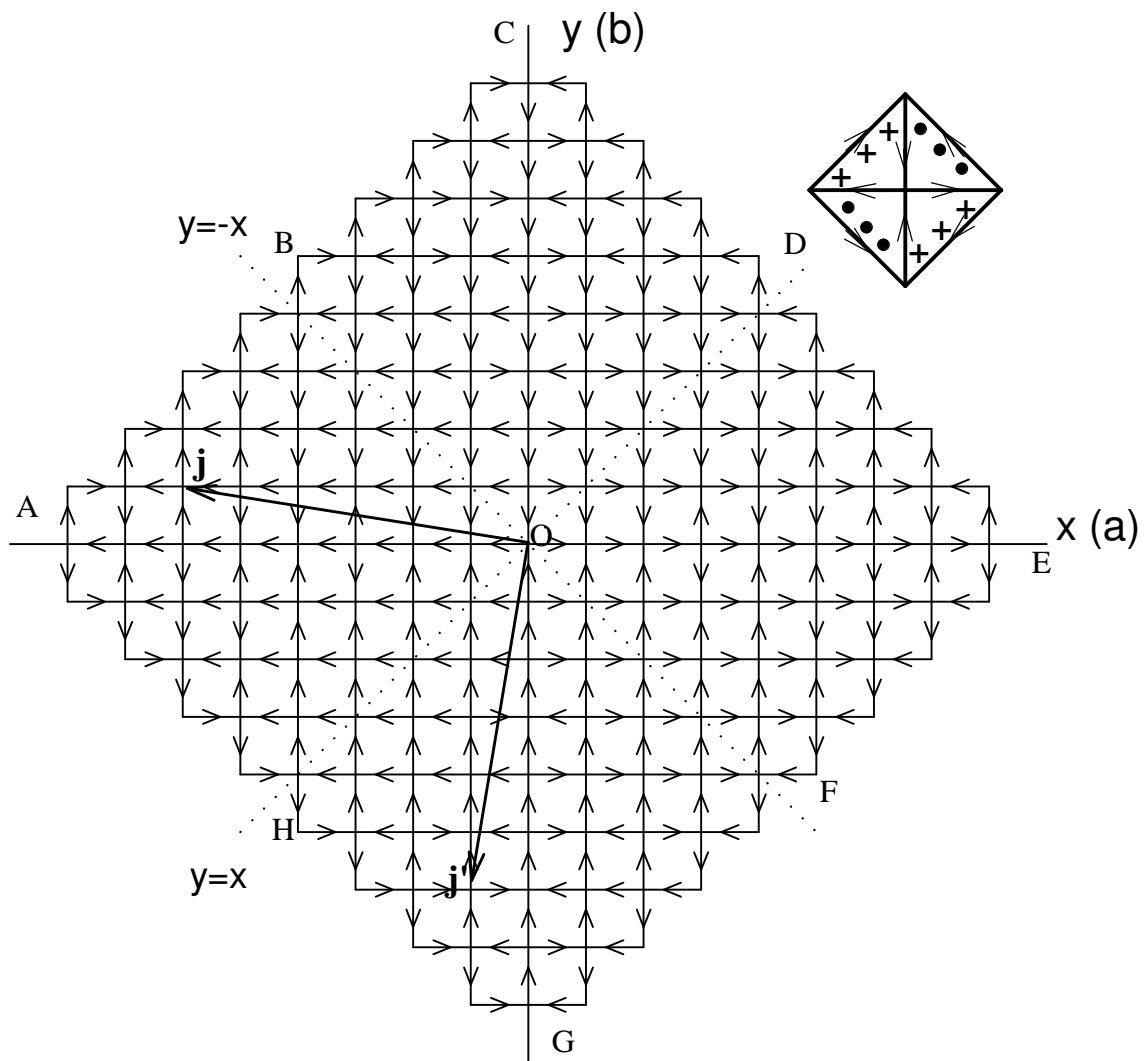


FIG. 1 Zhu et al.

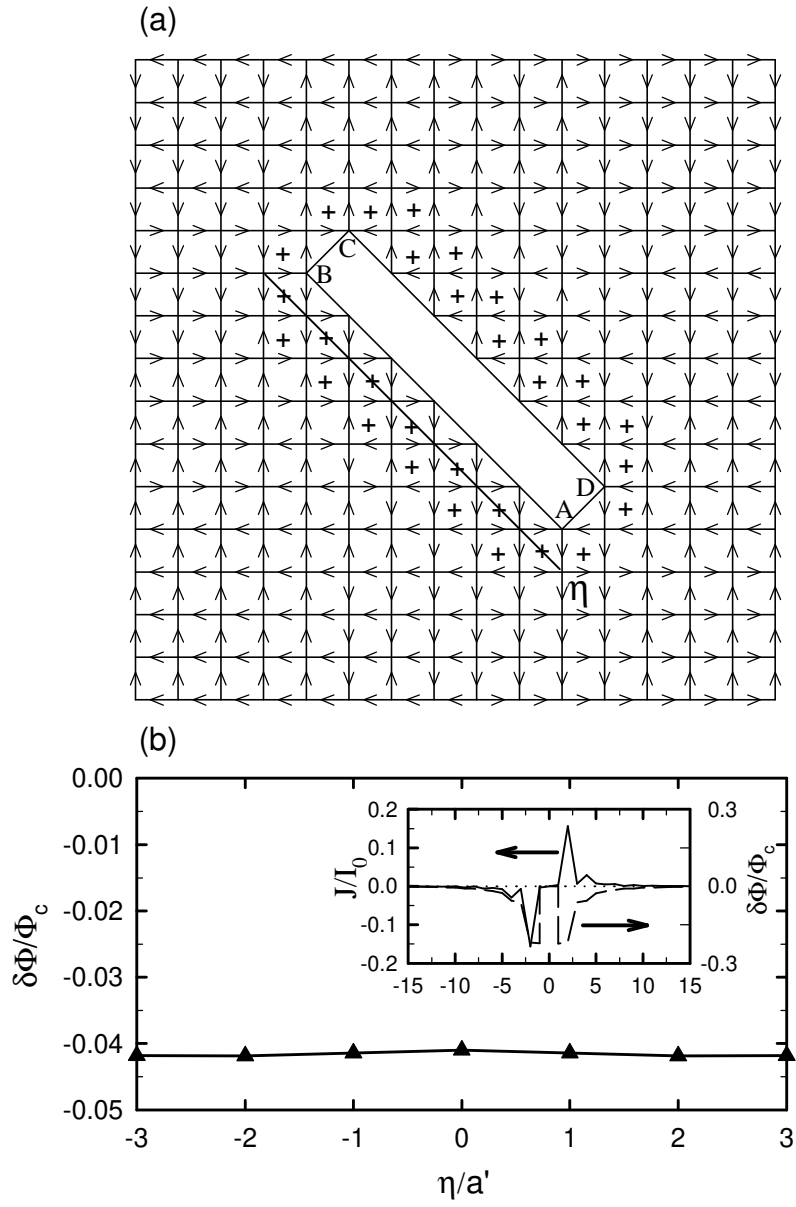


FIG. 2 Zhu et al.

